ISSN 2176-5480

22nd International Congress of Mechanical Engineering (COBEM 2013)
November 3-7, 2013, Ribeirão Preto, SP, Brazil

ADAPTIVE VISUAL SERVOING CONTROL IN 2D WITHOUT VELOCITY MEASUREMENTS

Maximiliano Bueno López
Jorge Eliécer Rangel Díaz
Facultad de Ingeniería. Universidad de La Salle. Cra. 2 No. 10-70, Bogotá D.C. Colombia.
maxbueno@unisalle.edu.co, jorangel@unisalle.edu.co

Marco Antonio Arteaga Pérez
Departamento de Control y Robótica. División de Ingeniería Eléctrica de la Facultad de Ingeniería. Universidad Nacional Autónoma de México. Apdo. Postal 70–256, México, D. F., 04510
marteagp@unam.mx

Abstract. *This paper considers the problem of position control of robot manipulators via visual servoing in presence of uncertainties associated with the robot dynamics and the vision system. Specifically, an adaptive algorithm is designed to compensate for the uncertainties associated with the mechanical model of the robot manipulator and the intrinsic parameters of the camera. We propose a control law which requires for implementation only joint and image coordinates, also a velocity observer is designed. This is achieved by combining a previous control algorithm designed originally to work Cartesian coordinates and an adaptive control law, to a version which uses image coordinates instead. Simulation results show the good performance of the complete system.*

Keywords: *Adaptive Control, Observer design, Visual Servoing, Tracking control.*

1. INTRODUCTION

The fixed camera strategy is a common approach in visual servoing for robot control. Usually, the objective consists in making that the manipulator end-effector follow a specified trajectory or reach a final point in the workspace (Chaumette and Hutchinson (2006), Chaumette and Hutchinson (2007)). When the manipulator is working in an unstructured environment, an useful approach is to employ a vision system for obtaining the end-effector position required by the controller (Hager and Corke (1996); Arteaga *et al.* (2009)). The use of cameras in the control of robot manipulators has increased in recent years due to the resulting good performance. Different techniques such as PID, adaptive and robust control and artificial intelligence can be combined with vision systems to solve the problem of tracking (Lizarralde *et al.* (2008); Lian *et al.* (2006); Weng *et al.* (2010)). The problem of designing adaptive control laws for rigid-robot manipulators that ensure asymptotic trajectory tracking has interested researchers for many years. The development of effective adaptive controllers represents an important step toward high-speed/precision robotic applications. Even in a well-structured industrial facility, robots uncertainty regarding the parameters describing the dynamic properties. Since the parameters are difficult to compute or measure, they limit the potential for robots to manipulate accurately objects of considerable size and weight. In Kelly *et al.* (2000) an alternative to camera calibration is proposed by carrying out vision system identification. To compensate for this parametric uncertainties, adaptive and robust controllers have been proposed (Kelly (1996), Zergeroglu and Behal (2001)). In Hsu *et al.* (2007) is presented a Lyapunov-based design of model-reference adaptive control (MRAC) for multiple-input multiple-output (MIMO) systems of uniform relative degree two. It consists of an extension of a known MRAC Lyapunov-based scheme for single-input single-output (SISO) plants with relative degree one or two. Only simulation results are shown. In Lizarralde *et al.* (2008) the direct adaptive control of planar robot manipulators through visual servoing is considered. A solution is developed for image-based visual systems to allow tracking of a desired trajectory, when both camera calibration and robot dynamics are uncertain. Also, only simulation results are presented. In Weng *et al.* (2010) a new adaptive controller for image-based tracking of a robot manipulator without visual velocity is introduced when the intrinsic and extrinsic parameters of the camera are not calibrated; to avoid poor performance caused by measurement errors of the visual velocity, image velocity estimation is proposed. Simulation results are given. In Liu *et al.* (2006) a stable adaptive tracking control of rigid-link electrically driven robot manipulators is presented in the presence of uncertainties in kinematics manipulator and actuator dynamics.

2. Preliminaries

The dynamics of a rigid robot arm with revolute joints can adequately be described by using the Euler–Lagrange equations of motion (Sciavicco and Siciliano (2000)), resulting in

$$\boldsymbol{H}(\boldsymbol{q})\ddot{\boldsymbol{q}} + \boldsymbol{C}(\boldsymbol{q},\dot{\boldsymbol{q}})\dot{\boldsymbol{q}} + \boldsymbol{D}\dot{\boldsymbol{q}} + \boldsymbol{g}(\boldsymbol{q}) = \boldsymbol{\tau} - \boldsymbol{\tau}_{\mathrm{p}}, \tag{1}$$

ISSN 2176-5480

where $\boldsymbol{q} \in \mathbb{R}^n$ is the vector of generalized joint coordinates, $\boldsymbol{H}(\boldsymbol{q}) \in \mathbb{R}^{n\times n}$ is the symmetric positive definite inertia matrix, $\boldsymbol{C}(\boldsymbol{q},\dot{\boldsymbol{q}})\dot{\boldsymbol{q}} \in \mathbb{R}^n$ is the vector of Coriolis and centrifugal torques, $\boldsymbol{g}(\boldsymbol{q}) \in \mathbb{R}^n$ is the vector of gravitational torques, $\boldsymbol{D} \in \mathbb{R}^{n\times n}$ is the positive semidefinite diagonal matrix accounting for joint viscous friction coefficients, $\boldsymbol{\tau} \in \mathbb{R}^n$ is the vector of torques acting at the joints. $\boldsymbol{\tau}_{\rm p} \in \mathbb{R}^n$ is the vector unknow bounded perturbances or nonlinear friction effects.

Let us denote the largest (smallest) eigenvalue of a matrix by $\lambda_{\max}(\cdot)$ ($\lambda_{\min}(\cdot)$). For a $n \times 1$ vector $\boldsymbol{x}$, we shall use the Euclidean norm $\|\boldsymbol{x}\| \triangleq \sqrt{\boldsymbol{x}^{\rm T}\boldsymbol{x}}$, while the norm of a $m \times n$ matrix $\boldsymbol{A}$ is the corresponding induced norm $\|\boldsymbol{A}\| \triangleq \sqrt{\lambda_{\max}(\boldsymbol{A}^{\rm T}\boldsymbol{A})}$. By recalling that revolute joints are considered, the following properties can be established:

Property 21. *It holds* $\lambda_{\rm h}\|\boldsymbol{x}\|^2 \leq \boldsymbol{x}^{\rm T}\boldsymbol{H}(\boldsymbol{q})\boldsymbol{x} \leq \lambda_{\rm H}\|\boldsymbol{x}\|^2 \quad \forall\, \boldsymbol{q},\ \boldsymbol{x} \in \mathbb{R}^n$, *and* $0 < \lambda_{\rm h} \leq \lambda_{\rm H} < \infty$, *given by*

$$\lambda_{\rm h} \triangleq \min_{\forall \boldsymbol{q}\in\mathbb{R}^n} \lambda_{\min}(\boldsymbol{H}(\boldsymbol{q}))$$

$$\lambda_{\rm H} \triangleq \max_{\forall \boldsymbol{q}\in\mathbb{R}^n} \lambda_{\max}(\boldsymbol{H}(\boldsymbol{q})).$$

Property 22. *With a proper definition of* $\boldsymbol{C}(\boldsymbol{q},\dot{\boldsymbol{q}})$, $\dot{\boldsymbol{H}}(\boldsymbol{q}) - 2\boldsymbol{C}(\boldsymbol{q},\dot{\boldsymbol{q}})$ *is skew symmetric.* △

Property 23. *It is satisfied* $\|\boldsymbol{C}(\boldsymbol{q},\boldsymbol{x})\| \leq k_{\rm c}\|\boldsymbol{x}\|$ *with* $0 < k_{\rm c} < \infty$, *and* $\forall\, \boldsymbol{x} \in \mathbb{R}^n$ △

Property 24. *The vector* $\boldsymbol{C}(\boldsymbol{q},\boldsymbol{x})\boldsymbol{y}$ *satisfies* $\boldsymbol{C}(\boldsymbol{q},\boldsymbol{x})\boldsymbol{y} = \boldsymbol{C}(\boldsymbol{q},\boldsymbol{y})\boldsymbol{x}$ *for all* $\boldsymbol{x},\boldsymbol{y} \in \mathbb{R}^n$ △

Property 25. *With a proper definition of the robot parameters, model (1) can be written as*

$$\boldsymbol{H}(\boldsymbol{q})\ddot{\boldsymbol{q}} \ + \ \boldsymbol{C}(\boldsymbol{q},\dot{\boldsymbol{q}})\dot{\boldsymbol{q}} + \boldsymbol{D}\dot{\boldsymbol{q}} + \boldsymbol{g}(\boldsymbol{q}) = \boldsymbol{\tau} + \boldsymbol{\tau}_{\rm p} = \boldsymbol{Y}(\boldsymbol{q},\dot{\boldsymbol{q}},\ddot{\boldsymbol{q}})\boldsymbol{\theta} - \boldsymbol{\tau}_{\rm p}, \tag{2}$$

where $\boldsymbol{Y}(\boldsymbol{q},\dot{\boldsymbol{q}},\ddot{\boldsymbol{q}}) \in \mathbb{R}^{n\times p}$ *is a regressor and* $\boldsymbol{\theta} \in \mathbb{R}^p$ *is a vector constant parameters.* △

In this paper, we will assume that the manipulator have two degrees of freedom planar manipulator, *i. e.* we have $n = 2$ in eq. (1). Then, the direct kinematics is a differentiable map $\boldsymbol{f}_{\rm k}(\boldsymbol{q}) : \mathbb{R}^2 \to \mathbb{R}^2$

$$\boldsymbol{x}_{\rm R} = \boldsymbol{f}_{\rm k}(\boldsymbol{q}), \tag{3}$$

relating the joint positions $\boldsymbol{q} \in \mathbb{R}^2$ to the Cartesian position $\boldsymbol{x}_{\rm R} \in \mathbb{R}^2$ of the centroid of a target attached at the arm end–effector. The output variable of the robotic system is the position $\boldsymbol{y} \in \mathbb{R}^2$ of the image feature, *i. e.* the position of the target in the computer screen.

These two quantities can be related by using Figure 1 as Pérez *et al.* (2008)

$$\boldsymbol{y} = \frac{\alpha\lambda}{O^{\rm C}_{\rm R3} - \lambda}\boldsymbol{R}_\phi \left[\boldsymbol{x}_{\rm R} - \begin{bmatrix} O^{\rm C}_{\rm R1} \\ O^{\rm C}_{\rm R2} \end{bmatrix}\right] + \begin{bmatrix} u_{\rm o} \\ v_{\rm o} \end{bmatrix} \triangleq \alpha_\lambda \boldsymbol{R}_\phi \left[\boldsymbol{x}_{\rm R} - \begin{bmatrix} O^{\rm C}_{\rm R1} \\ O^{\rm C}_{\rm R2} \end{bmatrix}\right] + \begin{bmatrix} u_{\rm o} \\ v_{\rm o} \end{bmatrix}, \tag{4}$$

where $\boldsymbol{O}^{\rm C}_{\rm R} = [\, O^{\rm C}_{\rm R1} \quad O^{\rm C}_{\rm R2} \quad O^{\rm C}_{\rm R3}\,]^T$ is the position of the origin of the camera frame $\Sigma_{\rm C}$ with respect to the robot frame $\Sigma_{\rm R}$, λ is the focal length, α is a conversion factor from meters to pixels, and $[\, u_{\rm o} \quad v_{\rm o}\,]^{\rm T}$ is the center offset. We assume that the camera image is parallel to the robot motion plane. $\boldsymbol{R}_\phi$ represents the orientation of the camera frame $\Sigma_{\rm C}$ with respect to the robot frame $\Sigma_{\rm R}$ and is given by

$$\boldsymbol{R}_\phi = \begin{bmatrix} \cos(\phi) & \sin(\phi) \\ \sin(\phi) & -\cos(\phi) \end{bmatrix}, \tag{5}$$

where $\phi \in \mathbb{R}$ is the rotation angle. Note that $\boldsymbol{R}_\phi^{-1} = \boldsymbol{R}_\phi^{\rm T} = \boldsymbol{R}_\phi$. From (4) one gets the differential perceptual kinematic model given by

$$\dot{\boldsymbol{y}} = \alpha_\lambda \boldsymbol{R}_\phi \boldsymbol{J}(\boldsymbol{q})\dot{\boldsymbol{q}} \qquad \Rightarrow \qquad \dot{\boldsymbol{q}} = \frac{1}{\alpha_\lambda}\boldsymbol{J}(\boldsymbol{q})^{-1}\boldsymbol{R}_\phi\dot{\boldsymbol{y}} \tag{6}$$

$$\ddot{\boldsymbol{y}} = \alpha_\lambda \boldsymbol{R}_\phi \boldsymbol{J}(\boldsymbol{q})\ddot{\boldsymbol{q}} + \alpha_\lambda \boldsymbol{R}_\phi \frac{\rm d}{{\rm d}t}\big(\boldsymbol{J}(\boldsymbol{q})\big)\dot{\boldsymbol{q}} \quad \Rightarrow$$

$$\ddot{\boldsymbol{q}} = \frac{1}{\alpha_\lambda}\boldsymbol{J}(\boldsymbol{q})^{-1}\boldsymbol{R}_\phi\ddot{\boldsymbol{y}} - \frac{1}{\alpha_\lambda}\boldsymbol{J}(\boldsymbol{q})^{-1}\dot{\boldsymbol{J}}(\boldsymbol{q}\boldsymbol{J}(\boldsymbol{q})^{-1}\boldsymbol{R}_\phi\dot{\boldsymbol{y}} \tag{7}$$

ISSN 2176-5480

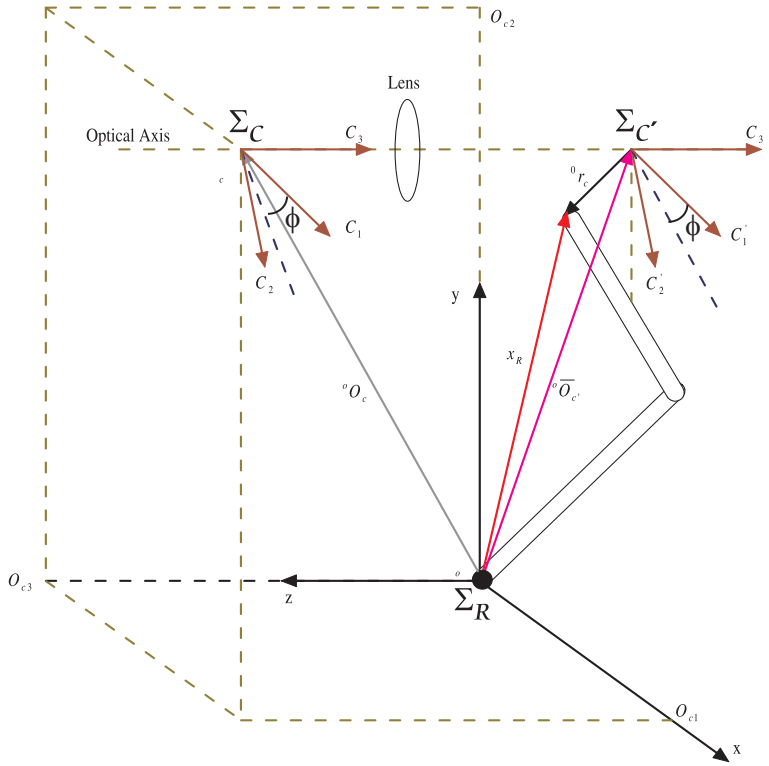

Figure 1. Reference System

where $\boldsymbol{J}(\boldsymbol{q}) = \partial \boldsymbol{f}_{\mathrm{k}}(\boldsymbol{q})/\partial \boldsymbol{q}$ is the so–called geometrical Jacobian matrix of the robot (Sciavicco et al., 2000), which satisfies the following well–known relationship

$$\dot{\boldsymbol{x}}_{\mathrm{R}} = \boldsymbol{J}(\boldsymbol{q})\dot{\boldsymbol{q}}. \tag{8}$$

Whenever the robot is not in a singularity, one also has the following relationship

$$\dot{\boldsymbol{q}} = \boldsymbol{J}^{-1}(\boldsymbol{q})\dot{\boldsymbol{x}}_{\mathrm{R}} \tag{9}$$

$$\ddot{\boldsymbol{q}} = \boldsymbol{J}^{-1}(\boldsymbol{q})\ddot{\boldsymbol{x}}_{\mathrm{R}} + \frac{\mathrm{d}}{\mathrm{dt}}\big(\boldsymbol{J}^{-1}(\boldsymbol{q})\big)\dot{\boldsymbol{x}}_{\mathrm{R}}, \tag{10}$$

Assumption 21. *The robot does not reach any singularity, so that* $\boldsymbol{J}^{-1}(\boldsymbol{q})$ *always exits.* △

By multiplying (1) by $\boldsymbol{R}_{\phi}\boldsymbol{J}^{-\mathrm{T}} = \boldsymbol{R}_{\phi}(\boldsymbol{J}^{-1}(\boldsymbol{q}))^{\mathrm{T}}$ and substituting (6-7) the robot model can be written in camera coordinates as

$$\boldsymbol{H}_{\mathrm{y}}\ddot{\boldsymbol{y}} + \boldsymbol{C}_{\mathrm{y}}(\boldsymbol{q},\dot{\boldsymbol{q}})\dot{\boldsymbol{y}} + \boldsymbol{D}_{\mathrm{y}}\dot{\boldsymbol{y}} + \boldsymbol{g}_{\mathrm{y}} = \boldsymbol{F} - \boldsymbol{\tau}_{\mathrm{y}} = \boldsymbol{Y}(\boldsymbol{y},\dot{\boldsymbol{y}},\ddot{\boldsymbol{y}})\boldsymbol{\theta} - \boldsymbol{\tau}_{\mathrm{y}} \tag{11}$$

where $\boldsymbol{\tau}_{\mathrm{y}}$ is the vector of unknown bounded perturbances in camera coordinates with

$$\boldsymbol{H}_{\mathrm{y}} = \frac{1}{\alpha_{\lambda}}\boldsymbol{R}_{\phi}\boldsymbol{J}^{-\mathrm{T}}\boldsymbol{H}(\boldsymbol{q})\boldsymbol{J}^{-1}\boldsymbol{R}_{\phi}, \tag{12}$$

$$\boldsymbol{C}_{\mathrm{y}}(\boldsymbol{q},\dot{\boldsymbol{q}}) = \frac{1}{\alpha_{\lambda}}\boldsymbol{R}_{\phi}\boldsymbol{J}^{-\mathrm{T}}\Big[\boldsymbol{C}(\boldsymbol{q},\dot{\boldsymbol{q}})\boldsymbol{J}^{-1}\boldsymbol{R}_{\phi} + \boldsymbol{H}(\boldsymbol{q})\boldsymbol{J}^{-1}\dot{\boldsymbol{J}}\boldsymbol{J}^{-1}\boldsymbol{R}_{\phi}\Big], \tag{13}$$

$$\boldsymbol{D}_{\mathrm{y}} = \frac{1}{\alpha_{\lambda}}\boldsymbol{R}_{\phi}\boldsymbol{J}^{-\mathrm{T}}\boldsymbol{D}\boldsymbol{J}^{-1}\boldsymbol{R}_{\phi}, \tag{14}$$

$$\boldsymbol{g}_{\mathrm{y}} = \boldsymbol{R}_{\phi}\boldsymbol{J}^{-\mathrm{T}}\boldsymbol{g}(\boldsymbol{q}), \tag{15}$$

$$\boldsymbol{F} = \boldsymbol{R}_{\phi}\boldsymbol{J}^{-\mathrm{T}}\boldsymbol{\tau} \tag{16}$$

Note that $\dot{\boldsymbol{J}}^{-1} = \frac{\mathrm{d}}{\mathrm{dt}}\big(\boldsymbol{J}^{-1}(\boldsymbol{q})\big)$. The robot model (11) keeps the same properties as the system in joint coordinates (Murray *et al.* (1994)).

ISSN 2176-5480

3. Adaptive visual servoing control

In this section, a tracking controller based on image coordinates will be designed. The task to be accomplished by the robot is to go from its initial position $\boldsymbol{y}(0)$ to a final position $\boldsymbol{y}_{\mathrm{f}}$ obtained and given respectively trough the camera image on the computer screen. Any soft desired trajectory $\boldsymbol{y}_{\mathrm{d}}$ with initial condition $\boldsymbol{y}_{\mathrm{d}}(0) = \boldsymbol{y}(0)$ and $\boldsymbol{y}_{\mathrm{d}}(\infty) = \boldsymbol{y}_{\mathrm{f}}$ can be used. For example, a velocity field or a five o six degree polynomial can be consider.

Furthermore, suppose that $\dot{\boldsymbol{y}}$ is not available so that an observer will be used. An estimate of $\boldsymbol{y}$ is given by $\hat{\boldsymbol{y}}$, and the observation error is given by

$$\boldsymbol{z} \triangleq \boldsymbol{y} - \hat{\boldsymbol{y}}. \tag{17}$$

We define the auxiliary variable

$$\dot{\boldsymbol{y}}_o \triangleq \dot{\hat{\boldsymbol{y}}} - \boldsymbol{\Lambda}_{\mathrm{z}}\boldsymbol{z}. \tag{18}$$

The corresponding observer is (Arteaga-Pérez and Kelly (2004))

$$\dot{\hat{\boldsymbol{y}}} = \dot{\hat{\boldsymbol{y}}}_o + \boldsymbol{\Lambda}_{\mathrm{z}}\boldsymbol{z} + k_d\boldsymbol{z}, \qquad \dot{\hat{\boldsymbol{y}}}(0) = \boldsymbol{0} \tag{19}$$

$$\dot{\hat{\boldsymbol{y}}}_o = \dot{\boldsymbol{y}}_{\mathrm{d}} - \boldsymbol{\Lambda}_{\mathrm{y}}(\hat{\boldsymbol{y}} - \boldsymbol{y}_{\mathrm{d}}) + \boldsymbol{s}_{\mathrm{d}} + k_d\boldsymbol{\Lambda}_{\mathrm{z}}\int_0^t \boldsymbol{z}(\vartheta)\mathrm{d}\vartheta \tag{20}$$

where $\boldsymbol{\Lambda}_{\mathrm{z}}, \boldsymbol{\Lambda}_{\mathrm{y}} \in \mathbb{R}^{2\times 2}$ are diagonal positive definite matrices, k_{d} is a positive constant and $\boldsymbol{s}_{\mathrm{d}} \in \mathbb{R}^2$ is aimed at improving transient response.

At this point, we recover the algorithm given in Arteaga-Pérez *et al.* (2006) and which was modified in Arteaga-Pérez *et al.* (2009) to be employed with image coordinates. First of all, in image coordinates the tracking error is given by

$$\Delta\boldsymbol{y} \triangleq \boldsymbol{y} - \boldsymbol{y}_{\mathrm{d}}. \tag{21}$$

To design the tracking controller, let us define

$$\dot{\boldsymbol{y}}_{\mathrm{r}} \triangleq \dot{\boldsymbol{y}}_{\mathrm{d}} - \boldsymbol{\Lambda}_{\mathrm{y}}(\hat{\boldsymbol{y}} - \boldsymbol{y}_{\mathrm{d}}) + \boldsymbol{s}_{\mathrm{d}} - \boldsymbol{K}_\gamma\boldsymbol{\sigma}, \tag{22}$$

$$\ddot{\boldsymbol{y}}_{\mathrm{r}} = \ddot{\boldsymbol{y}}_{\mathrm{d}} - \boldsymbol{\Lambda}_{\mathrm{y}}(\dot{\hat{\boldsymbol{y}}} - \dot{\boldsymbol{y}}_{\mathrm{d}}) - k\boldsymbol{s}_{\mathrm{d}} - \boldsymbol{K}_\gamma\dot{\boldsymbol{\sigma}}, \tag{23}$$

where $\boldsymbol{K}_\gamma \in \mathbb{R}^{2\times 2}$ is a diagonal positive definite matrix and $\boldsymbol{\sigma} \in \mathbb{R}^2$, with

$$\boldsymbol{s} = \dot{\hat{\boldsymbol{y}}} - \dot{\boldsymbol{y}}_{\mathrm{d}} + \boldsymbol{\Lambda}_{\mathrm{y}}(\hat{\boldsymbol{y}} - \boldsymbol{y}_{\mathrm{d}}) \triangleq \dot{\tilde{\boldsymbol{y}}} + \boldsymbol{\Lambda}_{\mathrm{y}}\bar{\boldsymbol{y}}, \tag{24}$$

$$\boldsymbol{s}_1 = \boldsymbol{s} - \boldsymbol{s}_{\mathrm{d}}, \tag{25}$$

$$\boldsymbol{s}_{\mathrm{d}} = \boldsymbol{s}(0)e^{-kt}, \tag{26}$$

$$\boldsymbol{\sigma} = \int_0^t \{\boldsymbol{K}_\beta\boldsymbol{s}_1(\vartheta) + \mathrm{sign}(\boldsymbol{s}_1(\vartheta))\}\,\mathrm{d}\vartheta, \tag{27}$$

where $\boldsymbol{\sigma}(0) = \boldsymbol{0}$, k is a positive constant, $\boldsymbol{K}_\beta \in \mathbb{R}^{2\times 2}$ is a diagonal positive definite matrix and

$$\mathrm{sign}(\boldsymbol{s}_1) \triangleq [\,\mathrm{sign}(s_{11}) \quad \cdots \quad \mathrm{sign}(s_{1n})\,]^{\mathrm{T}}, \tag{28}$$

with s_{1i} element of $\boldsymbol{s}_1$, $i = 1, \ldots, n$. Alternatively,

$$\dot{\boldsymbol{\sigma}} = \boldsymbol{K}_\beta\boldsymbol{s}_1 + \mathrm{sign}(\boldsymbol{s}_1) \tag{29}$$

can be used. Finally, the control law is given by

$$\boldsymbol{\tau} = -\boldsymbol{K}_{\mathrm{p}}\boldsymbol{J}^{\mathrm{T}}(\boldsymbol{q})\boldsymbol{R}_{\phi'}\boldsymbol{s}_{\mathrm{o}} \tag{30}$$

where

$$\boldsymbol{s}_{\mathrm{o}} \triangleq \dot{\boldsymbol{y}}_{\mathrm{o}} - \dot{\boldsymbol{y}}_{\mathrm{r}}. \tag{31}$$

Although in Arteaga-Pérez *et al.* (2009) it was shown that this law the control approach been tested experimentally successfully. Note that the algorithm garantees asyntotic stability, the experimental results show that fist movements diminish the system performance. This bad performance is due to a high sampling time. Since this is a hardware issue, in this paper we propose an adaptive algorithm to improve performance.Our main idea is as follows: the algorithm (17-30)

ISSN 2176-5480

will be used to deal with unknown dynamics and perturbances, while an adaptive algorithm will be designed to deal with the part of the system dynamics which can be written in a well-know structured model.

According to the Property 25, the vector $\boldsymbol{\theta} \in \mathbb{R}^p$ represents the robot model parameters. Suppose that $\hat{\boldsymbol{\theta}}$ represents a time varying vector of estimated parameters. Then, we propose to modify the control law (30) to

$$\begin{aligned} \boldsymbol{F} &= \hat{\boldsymbol{H}}_{\mathrm{y}}\ddot{\boldsymbol{y}}_{\mathrm{r}} + \hat{\boldsymbol{C}}_{\mathrm{y}}(\boldsymbol{y},\dot{\boldsymbol{y}}_{\mathrm{r}})\dot{\boldsymbol{y}}_{\mathrm{r}} + \hat{\boldsymbol{D}}_{\mathrm{y}}\dot{\boldsymbol{y}}_{\mathrm{r}} + \hat{\boldsymbol{g}}_{\mathrm{y}} - \boldsymbol{K}_{\mathrm{p}}\boldsymbol{R}_{\phi'}\boldsymbol{s}_{\mathrm{o}} && (32)\\ &= \boldsymbol{Y}_{\mathrm{a}}\hat{\boldsymbol{\theta}} - \boldsymbol{K}_{\mathrm{p}}\boldsymbol{R}_{\phi'}\boldsymbol{s}_{\mathrm{o}}, && (33)\end{aligned}$$

where $\hat{\boldsymbol{H}}$, $\hat{\boldsymbol{C}}$, $\hat{\boldsymbol{g}}$ one the matrices obtained from the matrices $\boldsymbol{H}$, $\boldsymbol{C}$, and $\boldsymbol{g}$ by substituting the estimated $\hat{\boldsymbol{\theta}}$ for the actual $\boldsymbol{\theta}$ Slotine and Li (1988) and $\boldsymbol{Y}_{\mathrm{a}} \triangleq \boldsymbol{Y}(\boldsymbol{y},\dot{\boldsymbol{y}}_{\mathrm{r}},\ddot{\boldsymbol{y}}_{\mathrm{r}}) \in \mathbb{R}^{n\times p}$. Also, it is

$$\boldsymbol{R}_{\phi'} = \begin{bmatrix} \cos(\phi') & \sin(\phi') \\ \sin(\phi') & -\cos(\phi') \end{bmatrix}, \tag{34}$$

with ϕ' an approximative value of ϕ. Furthermore

$$\boldsymbol{R}_{\tilde{\phi}} \triangleq \boldsymbol{R}_{\phi'}\boldsymbol{R}_{\phi} = \begin{bmatrix} \cos(\tilde{\phi}) & \sin(\tilde{\phi}) \\ -\sin(\tilde{\phi}) & \cos(\tilde{\phi}) \end{bmatrix} \tag{35}$$

where $\tilde{\phi} = \phi - \phi'$. For the implementation it is employed

$$\boldsymbol{\tau} = \boldsymbol{J}^{\mathrm{T}}(\boldsymbol{q})\boldsymbol{F}. \tag{36}$$

First all, to carry out the development we introduce

$$\begin{aligned} \boldsymbol{r} &\triangleq \dot{\boldsymbol{y}} - \dot{\boldsymbol{y}}_{\mathrm{o}} = \dot{\boldsymbol{z}} + \boldsymbol{\Lambda}_{\mathrm{z}}\boldsymbol{z}, && (37)\\ \boldsymbol{s}_{\mathrm{y}} &\triangleq \dot{\boldsymbol{y}} - \dot{\boldsymbol{y}}_{\mathrm{r}}. && (38)\end{aligned}$$

With these definitions, from (31) we have $\boldsymbol{s}_{\mathrm{o}} = \boldsymbol{s}_{\mathrm{y}} - \boldsymbol{r}$, which allows to rewrite the control law (33) as

$$\boldsymbol{F} = \boldsymbol{Y}_{\mathrm{a}}\hat{\boldsymbol{\theta}} - \boldsymbol{K}_{\mathrm{p}}\boldsymbol{R}_{\phi'}\boldsymbol{s}_{\mathrm{y}} + \boldsymbol{K}_{\mathrm{p}}\boldsymbol{R}_{\phi'}\boldsymbol{r} \tag{39}$$

o

$$\begin{aligned} \boldsymbol{F} &= \boldsymbol{H}_{\mathrm{y}}\ddot{\boldsymbol{y}}_{\mathrm{r}} + \boldsymbol{C}_{\mathrm{y}}(\boldsymbol{y},\dot{\boldsymbol{y}}_{\mathrm{r}})\dot{\boldsymbol{y}}_{\mathrm{r}} + \boldsymbol{D}_{\mathrm{y}}\dot{\boldsymbol{y}}_{\mathrm{r}} + \boldsymbol{g}_{\mathrm{y}} - \boldsymbol{K}_{\mathrm{p}}\boldsymbol{R}_{\phi'}\boldsymbol{s}_{\mathrm{y}} + \boldsymbol{K}_{\mathrm{p}}\boldsymbol{R}_{\phi'}\boldsymbol{r} && (40)\\ &\quad +(\hat{\boldsymbol{H}}_{\mathrm{y}} - \boldsymbol{H}_{\mathrm{y}})\ddot{\boldsymbol{y}}_{\mathrm{r}} + (\hat{\boldsymbol{C}}_{\mathrm{y}}(\boldsymbol{y},\dot{\boldsymbol{y}}_{\mathrm{r}}) - \boldsymbol{C}_{\mathrm{y}}(\boldsymbol{y},\dot{\boldsymbol{y}}_{\mathrm{r}}))\dot{\boldsymbol{y}}_{\mathrm{r}} + (\hat{\boldsymbol{D}}_{\mathrm{y}} - \boldsymbol{D}_{\mathrm{y}})\dot{\boldsymbol{y}}_{\mathrm{r}} + \hat{\boldsymbol{g}}_{\mathrm{y}} - \boldsymbol{g}_{\mathrm{y}} \\ &= \boldsymbol{H}_{\mathrm{y}}\ddot{\boldsymbol{y}}_{\mathrm{r}} + \boldsymbol{C}_{\mathrm{y}}(\boldsymbol{y},\dot{\boldsymbol{y}}_{\mathrm{r}})\dot{\boldsymbol{y}}_{\mathrm{r}} + \boldsymbol{D}_{\mathrm{y}}\dot{\boldsymbol{y}}_{\mathrm{r}} + \boldsymbol{g}_{\mathrm{y}} - \boldsymbol{K}_{\mathrm{p}}\boldsymbol{R}_{\phi'}\boldsymbol{s}_{\mathrm{y}} + \boldsymbol{K}_{\mathrm{p}}\boldsymbol{R}_{\phi'}\boldsymbol{r} + \boldsymbol{Y}_{\mathrm{a}}\tilde{\boldsymbol{\theta}}, && (41)\end{aligned}$$

where $\tilde{\boldsymbol{\theta}} = \hat{\boldsymbol{\theta}} - \boldsymbol{\theta}$. By taking into account that (see Property 24)

$$\boldsymbol{C}_{\mathrm{y}}(\boldsymbol{y},\dot{\boldsymbol{y}}_{\mathrm{r}})\dot{\boldsymbol{y}}_{\mathrm{r}} = \boldsymbol{C}_{\mathrm{y}}(\boldsymbol{y},\dot{\boldsymbol{y}} - (\dot{\boldsymbol{y}} - \dot{\boldsymbol{y}}_{\mathrm{r}}))\dot{\boldsymbol{y}}_{\mathrm{r}} = \boldsymbol{C}_{\mathrm{y}}(\boldsymbol{y},\dot{\boldsymbol{y}} - \boldsymbol{s}_{\mathrm{y}})\dot{\boldsymbol{y}}_{\mathrm{r}} = \boldsymbol{C}_{\mathrm{y}}(\boldsymbol{y},\dot{\boldsymbol{y}}) - \boldsymbol{C}_{\mathrm{y}}(\boldsymbol{y},\boldsymbol{s}_{\mathrm{y}})\dot{\boldsymbol{y}}_{\mathrm{r}}. \tag{42}$$

The tracking error closed loop dynamics is obtained by substituting (40),(42) in (11) to get

$$\boldsymbol{H}_{\mathrm{y}}\dot{\boldsymbol{s}}_{\mathrm{y}} + \boldsymbol{C}_{\mathrm{y}}(\boldsymbol{y},\dot{\boldsymbol{y}})\boldsymbol{s}_{\mathrm{y}} + \boldsymbol{K}_{\mathrm{DP}}\boldsymbol{s}_{\mathrm{y}} = \boldsymbol{K}_{\mathrm{p}}\boldsymbol{R}_{\phi'}\boldsymbol{r} + \boldsymbol{Y}_{\mathrm{a}}\tilde{\boldsymbol{\theta}} - \boldsymbol{\tau}_{\mathrm{y}} - \boldsymbol{C}_{\mathrm{y}}(\boldsymbol{y},\dot{\boldsymbol{y}}_{\mathrm{r}})\boldsymbol{s}_{\mathrm{y}}, \tag{43}$$

where $\boldsymbol{K}_{\mathrm{DP}} \triangleq \boldsymbol{D}_{\mathrm{y}} + \boldsymbol{K}_{\mathrm{p}}\boldsymbol{R}_{\phi'}$.

Defined the filtered input by $F_{\mathrm{f}} \triangleq W(s)F$ with $W(s) = \lambda_{\mathrm{f}}/(s+\lambda_{\mathrm{f}})$ and $\lambda_{\mathrm{f}} > 0$ (Arteaga-Pérez (2003)). The filtered regressor is given by $\boldsymbol{Y}_{\mathrm{f}}(\boldsymbol{y},\dot{\boldsymbol{y}}) \triangleq W(s)\boldsymbol{Y}(\boldsymbol{y},\dot{\boldsymbol{y}},\ddot{\boldsymbol{y}})$. Since $\dot{\boldsymbol{y}}$ is not available, the estimated filtered regressor is defined as $\hat{\boldsymbol{Y}}_{\mathrm{f}}(\boldsymbol{y},\hat{\dot{\boldsymbol{y}}}) = \boldsymbol{Y}_{\mathrm{f}}(\boldsymbol{y},\hat{\dot{\boldsymbol{y}}})$. For simplicity, $\boldsymbol{Y}_{\mathrm{f}}$ or $\boldsymbol{Y}_{\mathrm{f}}(\cdot)$ and $\hat{\boldsymbol{Y}}_{\mathrm{f}}$ or $\hat{\boldsymbol{Y}}_{\mathrm{f}}(\cdot)$ will be used here after as long as there is no confusion. Also define the prediction error as $\boldsymbol{\varepsilon} \triangleq \hat{\boldsymbol{Y}}_{\mathrm{f}}\hat{\boldsymbol{\theta}} - \boldsymbol{\tau}_{\mathrm{f}} = \hat{\boldsymbol{Y}}_{\mathrm{f}}\hat{\boldsymbol{\theta}} - \boldsymbol{Y}_{\mathrm{f}}\boldsymbol{\theta}$. The proposed adaptation algorithm is based on that given in Arteaga-Pérez (2003):

$$\begin{aligned} \dot{\hat{\boldsymbol{\theta}}}(t) &= -\boldsymbol{\Gamma}^{-1}\Big(\boldsymbol{Y}_{\mathrm{a}}^{\mathrm{T}}\boldsymbol{s}_y + \zeta_1\Big(\boldsymbol{h} + \zeta_0\hat{\boldsymbol{Y}}_{\mathrm{f}}^{\mathrm{T}}\boldsymbol{\varepsilon}\Big) - \boldsymbol{f}_{\mathrm{b}}\Big), && (44)\\ \dot{\boldsymbol{h}}(t) &= -\lambda\boldsymbol{h}(t) + \zeta_2\hat{\boldsymbol{Y}}_{\mathrm{f}}^{\mathrm{T}}\boldsymbol{\varepsilon} + \boldsymbol{Z}(t)\dot{\hat{\boldsymbol{\theta}}}(t), \qquad \boldsymbol{h}(0) = \boldsymbol{0} && (45)\\ \dot{\boldsymbol{Z}}(t) &= -\lambda\boldsymbol{Z}(t) + \zeta_2\hat{\boldsymbol{Y}}_{\mathrm{f}}^{\mathrm{T}}\hat{\boldsymbol{Y}}_{\mathrm{f}}, \qquad \boldsymbol{Z}(0) = \boldsymbol{0}. && (46)\\ & && (47)\end{aligned}$$

where $\boldsymbol{\Gamma} \in \mathbb{R}^{p\times p}$ is a diagonal positive definite matrix. In (44), $\theta_{\mathrm{m_i}} \leq \hat{\theta}_i(0) \leq \theta_{\mathrm{M_i}}$, where $\theta_{\mathrm{m_i}}$ and $\theta_{\mathrm{M_i}}$ are two constants which satisfy: $\theta_{\mathrm{m_i}} \leq \theta_i \leq \theta_{\mathrm{M_i}}$. Note that it is quite reasonable to assume that at least the sign of the parameter θ_i is

ISSN 2176-5480

known (say it is positive). In this case, the lower bound is simply 0. The upper bound can be tuned arbitrarily large. Also in (44)-(45), ζ_2, λ are positive constants. ζ_1 is given by

$$\zeta_1 = \alpha_1 \frac{\| \boldsymbol{Y}_{\mathrm{a}}^{\mathrm{T}} \boldsymbol{s}_{\mathrm{y}} \|}{\lambda_{\min}(\boldsymbol{P(t)}) + \epsilon_2} \cdot \frac{1}{\epsilon_1} + \alpha_2 \tag{48}$$

where α_2, ϵ_1 and ϵ_2 are positive constants and $\alpha_1 > 2$, with $\boldsymbol{P} \stackrel{\triangle}{=} \boldsymbol{Z}(t) + \zeta_1 \hat{\boldsymbol{Y}}_{\mathrm{f}}^{\mathrm{T}}(t) \hat{\boldsymbol{Y}}_{\mathrm{f}}(t)$. Define the columns of $\boldsymbol{Y}_{\mathrm{a}}$ and $\hat{\boldsymbol{Y}}_{\mathrm{f}}$ as $\boldsymbol{y}_{\mathrm{a}} \in \mathbb{R}^n$ and $\hat{\boldsymbol{y}}_{\mathrm{f}} \in \mathbb{R}^n$ respectively, for $i = 1, \cdots, p$. Since once $\hat{\boldsymbol{\theta}} < \boldsymbol{\theta}_{\mathrm{m_i}}$ or $\hat{\boldsymbol{\theta}} > \boldsymbol{\theta}_{\mathrm{M_i}}$ the sign of $\tilde{\boldsymbol{\theta}}_i$ is known, the *i*-th element of $\boldsymbol{f}_{\mathrm{b}}$ is defined by

$$f_{\mathrm{b_i}} \quad = \quad -\mathrm{sign}(\tilde{\theta}_{\mathrm{i}}) \cdot \rho_{\mathrm{i}} \cdot \delta_{\mathrm{i}} \mid \boldsymbol{y}_{\mathrm{a_i}}^{\mathrm{T}} \boldsymbol{s}_{\mathrm{y_i}} + \zeta_1 \Big(\boldsymbol{h}_{\mathrm{i}} + \zeta_0 \hat{\boldsymbol{y}}_{\mathrm{f_i}}^{\mathrm{T}} \boldsymbol{\varepsilon} \Big) \mid \tag{49}$$

with $i = 1, \cdots, p$. h_{i} the *i*-th element of $\boldsymbol{h}(t)$, $\rho_{\mathrm{i}} > 1$ and

$$\delta_{\mathrm{i}} = \begin{cases} \frac{\hat{\theta}_{\mathrm{i}} - \theta_{\mathrm{u_i}}}{\theta_{\mathrm{U_i}} - \theta_{\mathrm{u_i}}} & \text{if } \theta_{\mathrm{u_i}} \leq \hat{\theta}_{\mathrm{i}} \leq \theta_{\mathrm{U_i}}, \\ 0 & \text{if } \theta_{\mathrm{l_i}} < \hat{\theta}_{\mathrm{i}} < \theta_{\mathrm{u_i}}, \\ \frac{\theta_{\mathrm{l_i}} - \hat{\theta}_{\mathrm{i}}}{\theta_{\mathrm{l_i}} - \theta_{\mathrm{L_i}}} & \text{if } \theta_{\mathrm{L_i}} \leq \hat{\theta}_{\mathrm{i}} \leq \theta_{\mathrm{l_i}} \end{cases}$$

where $\theta_{\mathrm{L_i}}, \theta_{\mathrm{l_i}}, \theta_{\mathrm{u_i}}$ and $\theta_{\mathrm{U_i}}$ are constants satisfying $\theta_{\mathrm{L_i}} < \theta_{\mathrm{l_i}} < \theta_{\mathrm{m_i}}$ and $\theta_{\mathrm{M_i}} < \theta_{\mathrm{u_i}} < \theta_{\mathrm{U_i}}$. Note that $f_{\mathrm{b_i}}$ is zero if $\mathrm{sign}(\tilde{\theta}_{\mathrm{i}})$ is unknown. The dynamics of the observation error is given in Arteaga-Pérez *et al.* (2009) by

$$\boldsymbol{r} + k_{\mathrm{d}} \int_0^t \boldsymbol{r}(\vartheta) \mathrm{d}\vartheta = \Delta \dot{\boldsymbol{y}} + \boldsymbol{\Lambda}_{\mathrm{y}} (\hat{\boldsymbol{y}} - \boldsymbol{y}_{\mathrm{d}}) + \boldsymbol{s}_{\mathrm{d}}. \tag{50}$$

For the closed loop dynamics given by (38)–(37), we define the corresponding state variables

$$\boldsymbol{x} \stackrel{\triangle}{=} \begin{bmatrix} \boldsymbol{s}_{\mathrm{y}} \\ \boldsymbol{r} \end{bmatrix}. \tag{51}$$

Now, a theorem can be established.

Theorem 31. *Consider a singularity free desired trajectory $\boldsymbol{y}_{\mathrm{d}}$ with bounded first and second derivatives, with initial condition $\boldsymbol{y}(0)$ and the desired final value $\boldsymbol{y}_{\mathrm{f}}$. Then, for the control law (33) and proper combination of the gains k, k_{d}, $\boldsymbol{\Lambda}_{\mathrm{y}}$, $\boldsymbol{\Lambda}_{\mathrm{z}}$, $\boldsymbol{K}_{\beta}$, $\boldsymbol{K}_{\gamma}$,$\boldsymbol{K}_{\mathrm{p}}$ and $\boldsymbol{\Gamma}$ can always be found so that tracking and observation errors ($\Delta\dot{\boldsymbol{y}}$, $\Delta\boldsymbol{y}$, $\dot{\boldsymbol{z}}$, $\boldsymbol{z}$) are bounded and tend to zero as long as the following condition is satisfied $|\tilde{\phi}| < \frac{\pi}{2}$. Furthermore the parameter error $\tilde{\boldsymbol{\theta}}$ remain bounded.* △

A detailed mathematical development of the proof, together with the necessary conditions for the controller–observer gains, are given in Section 5.

Remark 31. *The proof that the estimated parameter $\hat{\theta}_{\mathrm{i}}$ remain bounded by $\theta_{\mathrm{L_i}} \leq \hat{\theta}_{\mathrm{i}} \leq \theta_{\mathrm{U_i}}$ is detailed in Arteaga-Pérez (2003).* △

4. Simulation results

We have carried out some expriments with the model of the manipulator A465 of *CRS Robotics*. It has six degrees of fredom, but we have used only 2 joint to have a planar robot. Also we employ a model of the camera fixed so that the optical axis is perpendicular to the robot planar workspace. In order to implement the control law it is necessary to have $\boldsymbol{y}$ available, which is obtained by calculating the centroid of the sphere that have been attached at the robot end-effector. The desired trajectory of the feature point is to trace the following circular trajectory

$$\boldsymbol{y}_d(t) = \begin{bmatrix} 60 \times \sin(0.2t) + 265 \\ -60 \times \cos(0.2t) + 185 \end{bmatrix} pixel \tag{52}$$

In Figure 2 actual, desired and estimated image coordinates are shown. The tracking and observation errors are show in Figures 3 and 4 respectively.

In Figure 5 it can be seen the path followed by the end effector in the image coordinates.

ISSN 2176-5480

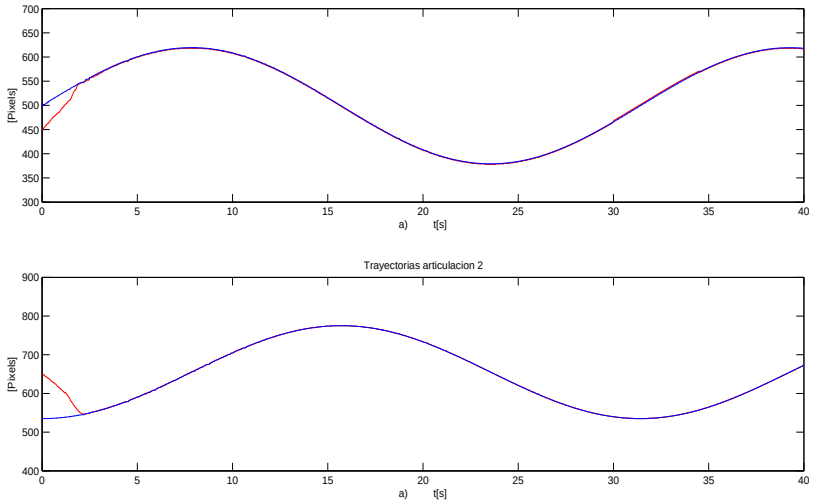

Figure 2. a) y_1 (——), $y_{\mathrm{d}1}$ (- - -) and $\hat{y}_1$ ($\cdots$). b) y_2 (——), $y_{\mathrm{d}2}$ (- - -) and $\hat{y}_2$ ($\cdots$). $\phi \approx 0°$.

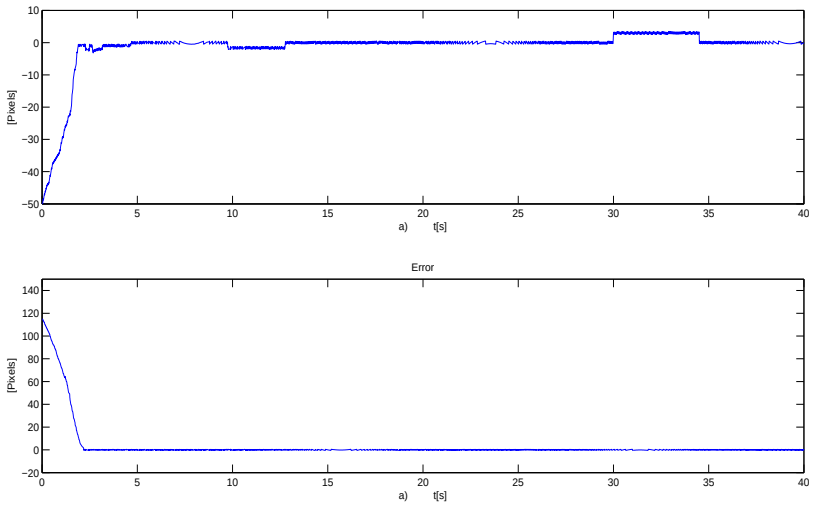

Figure 3. a) $\Delta\ y_1$. b) $\Delta\ y_2$. $\phi \approx 45°$.

5. Stability analysis

In this section, the proof of Theorem 3.1 is presented. As we noted in the introduction, this is a modification of the algorithm given in Arteaga-Pérez *et al.* (2006) with application to visual servoing, so that we just show the main issues of the proof for our current work, while the interested reader can look for details in the reference. Consider the following theorem and lemma.

Theorem 5.1. *(Khalil, 2002, pp. 172) Let $\mathbf{D} \subset \mathbf{R}^n$ be a domain that contains the origin and $V : [0, \infty) \times \mathbf{D} \to \mathbf{R}$ be a continuously differentiable function such that*

$$\alpha_1(\|\boldsymbol{x}\|) \leq V(t, \boldsymbol{x}) \quad \leq \quad \alpha_2(\|\boldsymbol{x}\|) \tag{53}$$

$$\frac{\partial V}{\partial t} + \frac{\partial V}{\partial \boldsymbol{x}} \boldsymbol{f}(t, \boldsymbol{x}) \quad \leq \quad -W_3(\boldsymbol{x}), \ \ \forall\, \|\boldsymbol{x}\| \geq \mu > 0, \tag{54}$$

$\forall\ t \geq 0$ and $\forall\ \boldsymbol{x} \in \mathbf{D}$, where α_1 and α_2 are class $\mathcal{K}$ functions, $W_3(\boldsymbol{x})$ is a continuous positive definite function and $\boldsymbol{f} : [0, \infty) \times \mathbf{D} \to \mathbf{R}^n$ is piecewise continuous in t and locally Lipschitz in $\boldsymbol{x}$ on $[0, \infty) \times \mathbf{D}$. Take $r > 0$ such that $\mathbf{B}_{\mathrm{r}} = \{\boldsymbol{x} \in \mathbf{R}^n | \|\boldsymbol{x}\| \leq r\} \subset \mathbf{D}$ and suppose that

$$\mu < \alpha_2^{-1}(\alpha_1(r)). \tag{55}$$

ISSN 2176-5480

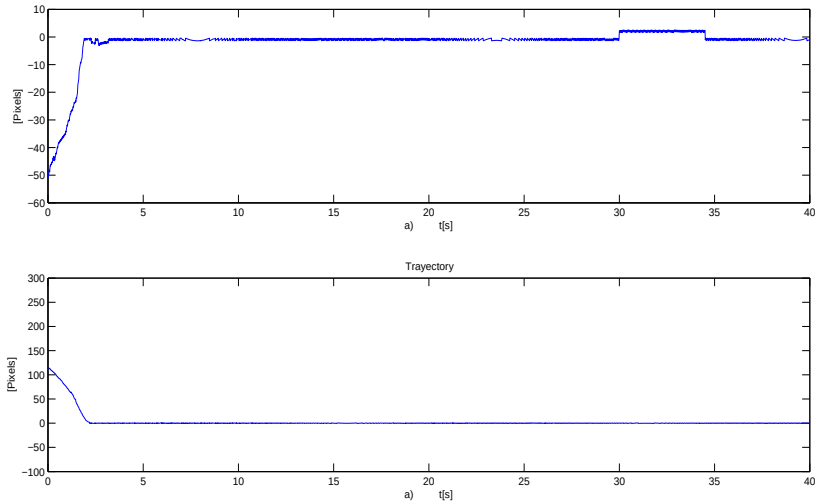

Figure 4. a) z_1. b) z_2. $\phi \approx 45°$.

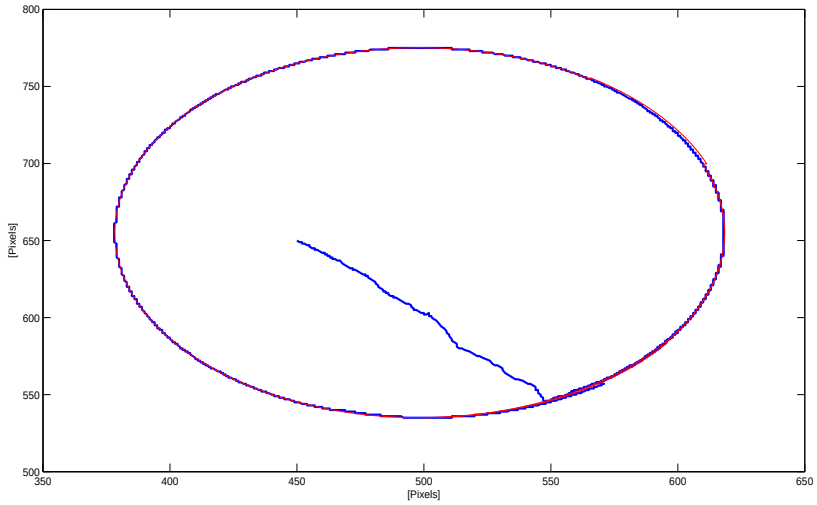

Figure 5. Path followed by the end effector

Then, there exits a class $\mathcal{KL}$ function β and for every initial state $\boldsymbol{x}(t_0)$, satisfying

$$\|\boldsymbol{x}(t_0)\| \leq \alpha_2^{-1}(\alpha_1(r)), \tag{56}$$

there is $T \geq 0$ (dependent on $\boldsymbol{x}(t_0)$ and μ) such that the solution of $\dot{\boldsymbol{x}} = \boldsymbol{f}(t, \boldsymbol{x})$ satisfies

$$\|\boldsymbol{x}\| \leq \beta(\|\boldsymbol{x}(t_0)\|, t - t_0), \quad \forall\, t_0 \leq t \leq t_0 + T \tag{57}$$

$$\|\boldsymbol{x}\| \leq \alpha_1^{-1}(\alpha_2(\mu)), \qquad \forall\, t \geq t_0 + T. \tag{58}$$

Moreover, if $\mathbf{D} = \mathbf{R}^n$ and α_1 belongs to class K_∞, then (57)–(58) hold for any initial state $\boldsymbol{x}(t_0)$, with no restriction on how large μ is. △

Lemma 5.1. *Arteaga-Pérez* et al. *(2006) Consider (27)–(28), and suppose you have the relationship*

$$\boldsymbol{s}_{\mathrm{i}} = \boldsymbol{s}_1 + \boldsymbol{K}_\gamma \boldsymbol{\sigma}. \tag{59}$$

If $\|\boldsymbol{s}_{\mathrm{i}}\| \leq \bar{s}_{\mathrm{i}} < \infty$ for all time, then $\boldsymbol{\sigma}$ and $\boldsymbol{s}_1$ are bounded for all time. Furthermore, a bound for $\boldsymbol{\sigma}$ is given by

$$\sigma_{\max} = \frac{2\left(\lambda_{\max}(\boldsymbol{K}_\beta)\bar{s}_{\mathrm{i}} + \sqrt{n}\right)}{\lambda_{\min}(\boldsymbol{K}_\beta \boldsymbol{K}_\gamma)}. \tag{60}$$

ISSN 2176-5480

$\triangle$

We prove Theorem 3.1 in three steps.

a) First of all, we show that if $\boldsymbol{x} = [\, \boldsymbol{s}_{\rm y}^{\rm T} \quad \boldsymbol{r}^{\rm T} \,]$ in (51) is bounded by $x_{\max}$, then any other signal is bounded. This proceeds as follows. Since from (37) one has the stable filter $\dot{\boldsymbol{z}} = -\boldsymbol{\Lambda}_{\rm z}\boldsymbol{z} + \boldsymbol{r}$, then both $\boldsymbol{z}$ and $\dot{\boldsymbol{z}}$ must be bounded. Then, from (22)–(25) and (38) one gets

$$\boldsymbol{s}_{\rm i} = \boldsymbol{s}_1 + \boldsymbol{K}_\gamma \boldsymbol{\sigma}, \tag{61}$$

with $\boldsymbol{s}_{\rm i} \stackrel{\triangle}{=} \boldsymbol{s}_{\rm y} - \dot{\boldsymbol{z}}$ bounded ($\boldsymbol{s}_{\rm y}$ is bounded because of its relationship with $\boldsymbol{s}_{\rm r}$ established in (38) and after Assumption 2.1). By applying Lemma 5.1 one concludes that $\boldsymbol{\sigma}$ and $\boldsymbol{s}_1$ are bounded. On the other hand, from (21), (22) and (38) one has

$$\Delta\dot{\boldsymbol{y}} + \boldsymbol{\Lambda}_{\rm y}\Delta\boldsymbol{y} = \boldsymbol{s}_{\rm y} + \boldsymbol{\Lambda}_{\rm y}\boldsymbol{z} + \boldsymbol{s}_{\rm d} - \boldsymbol{K}_\gamma\boldsymbol{\sigma}. \tag{62}$$

The dynamic equation for $\Delta\boldsymbol{y}$ represents a stable linear filter with bounded input, so that $\Delta\boldsymbol{y}$ and $\Delta\dot{\boldsymbol{y}}$ must be bounded. Now,

$$\dot{\boldsymbol{y}}_{\rm d} + k_1\boldsymbol{y}_{\rm d} = k_1\boldsymbol{y}_{\rm f} - \frac{k_0}{\|\tilde{\boldsymbol{y}}\| + \epsilon}\tilde{\boldsymbol{y}}. \tag{63}$$

Since $k_1 > 0$, we can conclude that both $\boldsymbol{y}_{\rm d}$ and $\dot{\boldsymbol{y}}_{\rm d}$ are bounded, because so is the righthand side of (63). Since of $\dot{\boldsymbol{y}}$ in (21), $\Delta\dot{\boldsymbol{y}} = \dot{\boldsymbol{y}} - \dot{\boldsymbol{y}}_{\rm d}$, $\boldsymbol{z}$ in (17) and $\dot{\boldsymbol{z}} = \dot{\boldsymbol{y}} - \dot{\hat{\boldsymbol{y}}}$ one concludes that $\boldsymbol{y}$ and $\dot{\boldsymbol{y}}$ (and $\hat{\boldsymbol{y}}$ and $\dot{\hat{\boldsymbol{y}}}$) are also bounded. On the other hand, from (4) it is

$$\dot{\boldsymbol{q}} = \frac{1}{\alpha_\lambda}\boldsymbol{J}^{-1}(\boldsymbol{q})\boldsymbol{R}_\phi\dot{\boldsymbol{y}}. \tag{64}$$

In view of Assumption 2.1, $\boldsymbol{q}$ must be bounded since no singularity has been reached and $\dot{\boldsymbol{q}}$ is bounded after (64). Furthermore, by taking the derivative of (63) and some norms it is

$$\|\ddot{\boldsymbol{y}}_{\rm d}\| \leq k_1\|\dot{\boldsymbol{y}}_{\rm d}\| + \frac{k_0}{\|\tilde{\boldsymbol{y}}\| + \epsilon}\|\dot{\tilde{\boldsymbol{y}}}\| + \frac{k_0\|\tilde{\boldsymbol{y}}\| \cdot \|\dot{\tilde{\boldsymbol{y}}}\|}{\left(\|\tilde{\boldsymbol{y}}\| + \epsilon\right)^2}. \tag{65}$$

This means that $\ddot{\boldsymbol{y}}_{\rm d}$ is bounded by recalling that $\tilde{\boldsymbol{y}} = \boldsymbol{y} - \boldsymbol{y}_{\rm f}$, with $\boldsymbol{y}_{\rm f}$ constant. Now, from (22) $\dot{\boldsymbol{y}}_{\rm r}$ is bounded and so is $\dot{\boldsymbol{q}}_{\rm r}$. Then we compute

$$\ddot{\boldsymbol{y}}_{\rm r} \quad = \quad \ddot{\boldsymbol{y}}_{\rm d} - \boldsymbol{\Lambda}_{\rm y}(\dot{\tilde{\boldsymbol{y}}} - \dot{\boldsymbol{y}}_{\rm d}) - k\boldsymbol{s}_{\rm d} - \boldsymbol{K}_\gamma\dot{\boldsymbol{\sigma}}, \tag{66}$$

which must be bounded because from (29) $\dot{\boldsymbol{\sigma}}$ is bounded. We also have

$$\ddot{\boldsymbol{q}}_{\rm r} = \frac{1}{\alpha_\lambda}\dot{\boldsymbol{J}}^{-1}(\boldsymbol{q})\boldsymbol{R}_\phi\dot{\boldsymbol{y}}_{\rm r} + \frac{1}{\alpha_\lambda}\boldsymbol{J}^{-1}(\boldsymbol{q})\boldsymbol{R}_\phi\ddot{\boldsymbol{y}}_{\rm r}, \tag{67}$$

where $\dot{\boldsymbol{J}}^{-1}(\boldsymbol{q}) = \frac{\rm d}{{\rm d}t}\boldsymbol{J}^{-1}(\boldsymbol{q})$. Then $\ddot{\boldsymbol{q}}_{\rm r}$ is bounded because the boundedness of $\dot{\boldsymbol{q}}$ ensures that of $\dot{\boldsymbol{J}}^{-1}(\boldsymbol{q})$. Also, $\dot{\boldsymbol{s}}_{\rm y}$ after (38) is bounded becouse $\ddot{\boldsymbol{y}}$ is bounded of (11) and by taking into account that $\boldsymbol{\tau}_{\rm y}$ is bounded by assumption, so $\boldsymbol{Y}_{\rm a} \stackrel{\triangle}{=} \boldsymbol{Y}(\boldsymbol{y}, \dot{\boldsymbol{y}}_{\rm r}, \ddot{\boldsymbol{y}}_{\rm r})$ is bounded.

To prove that the estimated parameter $\hat{\theta}_i$ will be bounded by $\theta_{{\rm L}i} \leq \hat{\theta}_i \leq \theta_{{\rm U}i}$, let us define the following function $V_{\rm f}(t) = \frac{1}{2}\gamma_i\tilde{\theta}_i^2$, whose derivative is given by

$$\dot{V}_{\rm f}(t) \quad = \quad -\tilde{\theta}_i\left(\boldsymbol{y}_{{\rm a}i}^{\rm T}\boldsymbol{s}_{{\rm y}_{\rm i}} + \zeta_1\left(h_i + \zeta_0\hat{\boldsymbol{y}}_{{\rm f}i}^{\rm T}\boldsymbol{\epsilon}\right)\right) + \tilde{\theta}_i f_{{\rm b}i}.$$

If $\theta_{{\rm l}i} < \theta_{{\rm m}i} \leq \hat{\theta}_i \leq \theta_{{\rm M}i} < \theta_{{\rm u}i}$ then $f_{{\rm b}i} \equiv 0$ and $\hat{\theta}_i$ is within the forseen bounds. But, if $\hat{\theta}_i < \theta_{{\rm l}i}$ or $\theta_{{\rm u}i} < \hat{\theta}_i$, then $f_{{\rm b}i}$ is different from zero. By taking (49) into account, one gets

$$\dot{V}_{\rm f}(t) \quad \leq \quad -(\rho_i - 1)|\tilde{\theta}_i|\left|\boldsymbol{y}_{{\rm a}i}^{\rm T}\boldsymbol{s}_{{\rm y}_{\rm i}} + \zeta_1\left(h_i + \zeta_0\hat{\boldsymbol{y}}_{{\rm f}i}^{\rm T}\boldsymbol{\epsilon}\right)\right|$$

ISSN 2176-5480

for the worst possible case $\hat{\theta}_i = \theta_{\mathrm{L}i}$ or $\hat{\theta}_i = \theta_{\mathrm{U}i}$ (since $\delta_i \equiv 1$ from (3)). Because $\rho_i > 1$ by definition, one concludes that $\theta_{\mathrm{L}i} \leq \hat{\theta}_i \leq \theta_{\mathrm{U}i}$ must be satisfied. At this point it is interesting to note that $\tilde{\boldsymbol{\theta}}^{\mathrm{T}} \boldsymbol{f}_{\mathrm{b}} = \boldsymbol{f}_{\mathrm{b}}^{\mathrm{T}} \tilde{\boldsymbol{\theta}} \leq 0$ $\forall\, t \geq 0$. It remains to prove that the region of attraction r given in (57) for the state $\boldsymbol{x}$ of (43) and (50), $\boldsymbol{x}$ will tend to the region μ in (58) in a finite time.

Furthermore $\hat{\boldsymbol{\theta}}$ is bounded of $\tilde{\boldsymbol{\theta}} + \boldsymbol{\theta} = \hat{\boldsymbol{\theta}}$. Note also that from (33) the input torque $\boldsymbol{F}$ is bounded, so that from (11) $\ddot{\boldsymbol{y}}$ must be bounded. It is also possible to compute from (4)

$$\ddot{\boldsymbol{y}} = \alpha_\lambda \boldsymbol{R}_\phi \dot{\boldsymbol{J}}(\boldsymbol{q})\dot{\boldsymbol{q}} + \alpha_\lambda \boldsymbol{R}_\phi \boldsymbol{J}(\boldsymbol{q})\ddot{\boldsymbol{q}}, \tag{68}$$

which turns out to be bounded as well. This also means that $\dot{\boldsymbol{r}}$ in (50) (and $\ddot{\boldsymbol{z}}$ and $\dddot{\hat{\boldsymbol{y}}}$ as a direct consequence) must be bounded. Finally, from (38) one has $\dot{\boldsymbol{s}}_{\mathrm{y}} = \ddot{\boldsymbol{y}} - \ddot{\boldsymbol{y}}_{\mathrm{r}}$ bounded, and so is $\dot{\boldsymbol{s}}_1$ after (25). Then, $\dot{\boldsymbol{s}}_{\mathrm{i}}$ is bounded as well after (61).

b) The next step is to show that, with a proper choice of gains, one can actually achieve $\|\boldsymbol{x}\| \leq x_{\max}$. We consider for simplicity $x_{\max}$ as a given value. Now define

$$V(\boldsymbol{x}) = \frac{1}{2}\boldsymbol{x}^{\mathrm{T}} \boldsymbol{M} \boldsymbol{x}, \tag{69}$$

with $\boldsymbol{M} \triangleq$ block diag $\{\, \boldsymbol{H}_{\mathrm{y}} \quad \boldsymbol{I} \,\}$. After Property 2.1 it satisfies

$$\lambda_1 \|\boldsymbol{x}\|^2 \leq V(\boldsymbol{x}) \leq \lambda_2 \|\boldsymbol{x}\|^2, \tag{70}$$

with

$$\lambda_1 \triangleq \frac{1}{2} \min_{\forall \boldsymbol{q} \in \mathbf{R}^2} \lambda_{\min}(\boldsymbol{M}(\boldsymbol{q})) \tag{71}$$

$$\lambda_2 \triangleq \frac{1}{2} \max_{\forall \boldsymbol{q} \in \mathbf{R}^2} \lambda_{\max}(\boldsymbol{M}(\boldsymbol{q})). \tag{72}$$

Now we use $V(\boldsymbol{x})$ in (69) and Theorem 5.1, with $\alpha_1 = \lambda_1 \|\boldsymbol{x}\|^2$ and $\alpha_2 = \lambda_2 \|\boldsymbol{x}\|^2$. By using Property 2.2, the derivative of V along (38) and (37) is given by

$$\begin{aligned} \dot{V} \;=\; & -\boldsymbol{s}_{\mathrm{y}}^{\mathrm{T}} \boldsymbol{K}_{\mathrm{DP}} \boldsymbol{s}_{\mathrm{y}} - k_{\mathrm{d}} \boldsymbol{r}^{\mathrm{T}} \boldsymbol{r} + \boldsymbol{s}_{\mathrm{y}}^{\mathrm{T}} \boldsymbol{K}_{\mathrm{p}} \boldsymbol{R}_{\phi'} \boldsymbol{r} + \boldsymbol{r}^{\mathrm{T}} \left\{ \Delta \ddot{\boldsymbol{y}} + \boldsymbol{\Lambda}_{\mathrm{y}} (\dot{\hat{\boldsymbol{y}}} - \dot{\boldsymbol{y}}_{\mathrm{d}}) + k \boldsymbol{s}_{\mathrm{d}} \right\} \\ & + \boldsymbol{s}_{\mathrm{y}}^{\mathrm{T}} \boldsymbol{Y}_{\mathrm{a}} \tilde{\boldsymbol{\theta}} - \boldsymbol{s}_{\mathrm{y}}^{\mathrm{T}} \boldsymbol{\tau}_{\mathrm{y}} - \boldsymbol{s}_{\mathrm{y}}^{\mathrm{T}} \boldsymbol{C}_{\mathrm{y}}(\boldsymbol{y}, \dot{\boldsymbol{y}}_{\mathrm{r}}) \boldsymbol{s}_{\mathrm{y}}, \end{aligned} \tag{73}$$

While V is positive definite for all $\boldsymbol{x} \in \mathbf{R}^{2n}$, to apply Theorem 5.1 it is necessary to find a region $\mathbf{D}$ for which (54) be satisfied. We define

$$\mathbf{D} \triangleq \left\{ \boldsymbol{x} \in \mathbf{R}^{2n} | \|\boldsymbol{x}\| \leq x_{\max} \right\}. \tag{74}$$

In this region, as shown in item a), bounds can be found so that one can define

$$c_1 \triangleq \max_{\forall \boldsymbol{q} \in \mathbf{R}^2} \|\boldsymbol{R}_{\phi'}\| \tag{75}$$

$$\mu_1 \triangleq \max_{\forall \boldsymbol{x} \in \mathbf{R}^{2n}} \|\Delta \ddot{\boldsymbol{y}} + \boldsymbol{\Lambda}_{\mathrm{y}} (\dot{\hat{\boldsymbol{y}}} - \dot{\boldsymbol{y}}_{\mathrm{d}}) + k \boldsymbol{s}_{\mathrm{d}}\| \tag{76}$$

$$\mu_2 \triangleq \boldsymbol{C}_{\mathrm{y}}(\boldsymbol{y}, \dot{\boldsymbol{y}}_{\mathrm{r}}) = k_{\mathrm{c}} \max_{\forall \boldsymbol{x} \in \mathbf{R}^{2n}} \|\dot{\boldsymbol{y}}_{\mathrm{d}} - \boldsymbol{\Lambda}_{\mathrm{y}} (\hat{\boldsymbol{y}} - \boldsymbol{y}_{\mathrm{d}}) + \boldsymbol{s}_{\mathrm{d}} - \boldsymbol{K}_\gamma \boldsymbol{\sigma}\| \tag{77}$$

Clearly, since $\|\boldsymbol{Y}_{\mathrm{a}} \tilde{\boldsymbol{\theta}}\|$, $\|\boldsymbol{\tau}_{\mathrm{y}}\|$, for $\|\boldsymbol{x}\| \leq \boldsymbol{x}_{\max}$ there exists a bound such that

$$\|\boldsymbol{Y}_{\mathrm{a}} \tilde{\boldsymbol{\theta}}\| \leq \mu_{\mathrm{a}} \tag{78}$$

$$\|\boldsymbol{\tau}_{\mathrm{y}}\| \leq \mu_{\mathrm{y}}, \tag{79}$$

ISSN 2176-5480

Thus, (73) can be computed to satisfy

$$\begin{aligned}\dot{V} &\leq -\lambda_{\min}(\bar{\boldsymbol{K}}_{\mathrm{p}})\|\boldsymbol{s}_{\mathrm{y}}\|^2 - k_{\mathrm{d}}\|\boldsymbol{r}\|^2 + \lambda_{\max}(\boldsymbol{K}_{\mathrm{p}})c_1\|\boldsymbol{s}_{\mathrm{y}}\|\|\boldsymbol{r}\| + \mu_1\|\boldsymbol{r}\| - \mu_2\|\boldsymbol{s}_{\mathrm{y}}\|^2 \\ &\quad +\mu_{\mathrm{a}}\|\boldsymbol{s}_{\mathrm{y}}\| + \mu_{\mathrm{y}}\|\boldsymbol{s}_{\mathrm{y}}\| \\ &\leq -\lambda_{\min}(\bar{\boldsymbol{K}}_{\mathrm{p}})\|\boldsymbol{s}_{\mathrm{y}}\|^2 - \mu_2\|\boldsymbol{s}_{\mathrm{y}}\|^2 - k_{\mathrm{d}}\|\boldsymbol{r}\|^2 + \lambda_{\max}(\boldsymbol{K}_{\mathrm{p}})c_1\|\boldsymbol{s}_{\mathrm{y}}\|\|\boldsymbol{r}\| + \alpha\|\boldsymbol{y}\|.\end{aligned} \tag{80}$$

where $\alpha \triangleq \mu_1 + \mu_{\mathrm{a}} + \mu_{\mathrm{y}}$. To achieve (54), we propose to choose

$$\lambda_{\min}(\boldsymbol{K}_{\mathrm{p}}) + \mu_2 \geq 1 + \delta \tag{81}$$

$$k_{\mathrm{d}} \geq \delta + \frac{1}{4}\lambda^2_{\max}(\boldsymbol{K}_{\mathrm{p}})c_1^2 \tag{82}$$

with $\delta > 0$,to get

$$\dot{V} \leq -\delta\|\boldsymbol{s}_{\mathrm{y}}\|^2 - \delta\|\boldsymbol{r}\|^2 + \alpha\|\boldsymbol{x}\| \tag{83}$$

$$\leq -\frac{1}{2}\delta\|\boldsymbol{x}\|^2 - \left(\frac{1}{2}\delta\|\boldsymbol{x}\|^2 - \alpha\|\boldsymbol{x}\|\right) \tag{84}$$

A conservative value for μ can be defined as

$$\mu \triangleq \frac{2\alpha}{\delta} < \sqrt{\frac{\lambda_1}{\lambda_2}}\, y_{\max}. \tag{85}$$

After having shown that it is actually possible to satisfy 55), we have that if $\|\boldsymbol{x}\| \geq \mu > 0$, then it is

$$\dot{V} \leq -\frac{1}{2}\delta\|\boldsymbol{x}\|^2 \triangleq -W_3(\boldsymbol{x}), \tag{86}$$

which allows to employ Theorem 5.1 and to conclude this part of the proof. Note that the final bound (58) becomes

$$\|\boldsymbol{x}\| \leq \sqrt{\frac{\lambda_2}{\lambda_1}}\,\mu. \tag{87}$$

Sometimes, this is referred to as practical stability since all error variables of the system can be made arbitrarily small.

c) Till now we have shown that $\boldsymbol{y}$ is bounded. We still have to prove that tracking and observation errors tend to zero. By defining $V_1 = \frac{1}{2}\boldsymbol{s}_1^{\mathrm{T}}\boldsymbol{s}_1 = \frac{1}{2}\|\boldsymbol{s}_1\|^2$, from (29) and (61) one obtains

$$\frac{\mathrm{d}\|\boldsymbol{s}_1\|}{\mathrm{d}t} \leq -\psi, \tag{88}$$

with $\psi \triangleq (\lambda_{\min}(\boldsymbol{K}_\gamma) - s_{\mathrm{ipmax}})$ and $\|\dot{\boldsymbol{s}}_{\mathrm{i}}\| < s_{\mathrm{ipmax}}\ \forall\, t$. If $\lambda_{\min}(\boldsymbol{K}_\gamma)$ can be chosen arbitrarily large, then $\psi > 0$. To show that this is in fact possible, from Lemma 5.1 a bound for $\boldsymbol{\sigma}$ is given by (60). Then, to simplify our discussion we can assume that $\boldsymbol{K}_\beta = \boldsymbol{I}k_\beta$ and $\boldsymbol{K}_\gamma = \boldsymbol{I}k_\gamma$, with $k_\beta, k_\gamma > 0$, so that from (60) we have[1]

$$k_\gamma\|\boldsymbol{\sigma}\| \leq 2s_{\mathrm{ipmax}} + \frac{2\sqrt{n}}{k_\beta}. \tag{89}$$

Note that whenever used in our control–observer scheme, $\boldsymbol{\sigma}$ never appears alone but instead one has $\boldsymbol{K}_\gamma\boldsymbol{\sigma}$ (or $k_\gamma\boldsymbol{\sigma}$ for our particular case). Equation (89) means that k_γ can be made arbitrarily large while keeping $\boldsymbol{K}_\gamma\boldsymbol{\sigma}$ bounded. The same can be said for k_β. In turns this implies that one can always set $\boldsymbol{\theta} > 0$. Then, it can be shown that $\boldsymbol{s}_1 = \boldsymbol{0}$ in a finite time t_{r}, so that from (24)–(26) one gets

$$\boldsymbol{s} = \dot{\bar{\boldsymbol{y}}} + \boldsymbol{\Lambda}_{\mathrm{y}}\bar{\boldsymbol{y}} = \boldsymbol{s}_{\mathrm{d}} = \boldsymbol{s}(0)e^{-kt}, \tag{90}$$

with $\bar{\boldsymbol{y}} = \hat{\boldsymbol{y}} - \boldsymbol{y}_{\mathrm{d}}$. Since e^{-kt} tends to zero, we have that $\boldsymbol{s} \to \boldsymbol{0}$. This in turn means that $\bar{\boldsymbol{y}}$ and $\dot{\bar{\boldsymbol{y}}}$ will tend to zero. Note that if $\bar{\boldsymbol{y}} = \boldsymbol{0}$ and $\dot{\bar{\boldsymbol{y}}} = \boldsymbol{0}$, then $\Delta\boldsymbol{y} = \boldsymbol{z}$ and $\Delta\dot{\boldsymbol{y}} = \dot{\boldsymbol{z}}$ for a large enough time. Hence, (50) and using (37) one has

$$(k_{\mathrm{d}}\boldsymbol{I} + \boldsymbol{\Lambda}_{\mathrm{z}})\dot{\boldsymbol{z}} + k_{\mathrm{d}}\boldsymbol{\Lambda}_{\mathrm{z}}\boldsymbol{z} = \boldsymbol{0}. \tag{91}$$

Equation (91) represents a stable linear filter for $\boldsymbol{z}$, so that $\boldsymbol{z}$ and $\dot{\boldsymbol{z}}$ tend to zero. This in turn means that $\Delta\boldsymbol{y}$ and $\Delta\dot{\boldsymbol{y}}$ do tend to zero as well.

[1]Note that as stated in Theorem 3.1 we just have to find a proper combination for $\boldsymbol{K}_\beta$ and $\boldsymbol{K}_\gamma$, so that we chose the simplest case for the proof.

ISSN 2176-5480

6. Conclusions

In this paper we present an adaptive control with velocity observer for tracking in image coordinates. Only image coordinates and joint position is required for implementation. To test the theory, simulation results have been carried out which show a good performance of the proposed method. According to the simulation results, the two coordinates of the image used converge to the desired value in a good time, considering that this is a servovisual control which also include friction effects. The adaptive control strategy proves to be very useful in robotics because the number of uncertain parameters is very high.

7. REFERENCES

Arteaga, M., Bueno, M. and Espinoza, A., 2009. "A simple approach for 2D visual servoing". In *18th IEEE International Conference on Control Applications. Part of 2009 IEEE Multi-conference on Systems and Control, Saint Petersburg, Russia*. pp. 1692–1699.

Arteaga-Pérez, M.A., 2003. "Robot control and parameter estimation with only joint position measurements". *Automatica*, Vol. 39, pp. 67–73.

Arteaga-Pérez, M.A., Castillo-Sánchez, A.M. and Parra-Vega, V., 2006. "Cartesian control of robots without dynamic model and observer design". *Automatica*, Vol. 42, pp. 473–480.

Arteaga-Pérez, M.A. and Kelly, R., 2004. "Robot control without velocity measurements: New theory and experimental results". *IEEE Transactions on Robotics and Automation*, Vol. 20, No. 2, pp. 297–308.

Arteaga-Pérez, M.A., Maximiliano, B.L. and Espinosa, A., 2009. "A simple approach for 2d visual servoing". In *IEEE Control Systems Society CSS09*. Saint Petersburg, Russia, pp. 1557–1562.

Chaumette, F. and Hutchinson, S., 2006. "Visual servo control, Part I: Basic approaches". *IEEE Robotics and Automation Magazine*, Vol. 13, No. 4, pp. 82–90.

Chaumette, F. and Hutchinson, S., 2007. "Visual servo control, Part II: Advanced Approaches". *IEEE Robotics and Automation Magazine*, Vol. 14, No. 1, pp. 109–118.

Hager, G. and Corke, P., 1996. "A tutorial on visual servo control". *IEEE Transactions on Robotics and Automation*.

Hsu, L., Costa, R. and Lizarralde, F., 2007. "Lyapunov/Passivity-based adaptive control of relative degree two MIMO systems with an application to visual servoing". *IEEE Transactions on Automatic Control*, Vol. 52, No. 2, pp. 364–371.

Kelly, R., 1996. "Robust asymptotically stable visual servoing of planar robots". *IEEE Transactions on Robotics and Automation*, Vol. 12, No. 5, pp. 759–766.

Kelly, R., Llamas, J. and Campa, R., 2000. "A measurement procedure for viscous and Coulomb friction". *IEEE Transactions on Instrumentation and Measurement*, Vol. 49, No. 4, pp. 857–861.

Khalil, H.K., 2002. *Nonlinear Systems, 3rd ed*. Prentice–Hall, Upper Saddle River, New Jersey. U .S. A.

Lian, K.Y., Tu, H.W. and Liou, J.J., 2006. "Stability conditions for LMI-based fuzzy control from viewpoint of membership functions". *IEEE Transactions on Fuzzy Systems*, Vol. 14, No. 6, pp. 874–884.

Liu, C., Cheah, C. and Slotine, J., 2006. "Adaptive Jacobian Tracking control of rigid-link electrically driven robots based on visual task-space information". *Automatica*, Vol. 42, No. 9, pp. 1491–1501.

Lizarralde, F., Hsu, L. and Costa, R., 2008. "Adaptive visual servoing of robot manipulators without measuring the image velocity". In *17th World Congress The International Federation of Automatic Control. Seoul, Korea*.

Murray, R.M., Li, Z. and Sastry, S.S., 1994. *A Mathematical Introduction to Robotic Manipulation*. CRC Press, Boca Raton, Florida, U. S. A.

Pérez, R.R., Arteaga-Pérez, M.A., Kelly, R. and Espinosa, A., 2008. "On output regulation of direct visual servoing via velocity fields". *International Journal of Control*.

Sciavicco, L. and Siciliano, B., 2000. *Modeling and Control of Robot Manipulators, 2nd ed*. Springer–Verlag, London, Great Britain.

Slotine, J.J.E. and Li, W., 1988. "Adaptive manipulator control: A case study". *IEEE Transactions on Automatic Control*, Vol. 33, No. 11, pp. 995–1003.

Weng, H., Liu, Y.H. and Chen, W., 2010. "Uncalibrated visual tracking control without visual velocity". *IEEE Transactions on Control Systems Technology*, Vol. 18, No. 6, pp. 1359–1370.

Zergeroglu, E., D.D.M.d.Q. and Behal, A., 2001. "Vision-based nonlinear tracking controllers with uncertain robot-camera parameters". *Journal of Robotic Systems*, Vol. 20, pp. 93–106.

8. RESPONSIBILITY NOTICE

The authors are the only responsible for the printed material included in this paper.